Available online at www.sciencedirect.com
SCIENCE DIRECT®

Journal of Catalysis 222 (2004) 545–557

JOURNAL OF CATALYSIS

www.elsevier.com/locate/jcat

Dehydrogenation of cyclohexanol on copper-containing catalysts

II. The pathways of the cyclohexanol dehydrogenation reaction to cyclohexanone on copper-active sites in oxidation state Cu^0 and Cu^+

V.Z. Fridman,* A.A. Davydov, and K. Titievsky[1]

Xenonum Scientific Services, Jenks, OK, USA

Received 19 September 2003; revised 15 December 2003; accepted 26 December 2003

Abstract

The mechanism of cyclohexanol and cyclohexanone adsorption and the kinetics and mechanism of cyclohexanol dehydrogenation to cyclohexanone over Cu^0 catalysts (on Cu–Mg) and Cu^+ catalysts (on Cu–Zn–Al) were studied by IR spectroscopy and kinetic methods. In situ IR spectroscopy data demonstrated that cyclohexanol is adsorbed onto monovalent copper at room temperature, forming molecularly adsorbed cyclohexanol and cyclohexanol alcoholate of Cu^+. Cyclohexanol alcoholate species were considered as intermediates for cyclohexanone formation on monovalent copper sites. Unlike in the case of Cu^+, the dissociative adsorption of cyclohexanol on Cu^0 was observed only at temperatures of 50 °C or higher. Cyclohexanol adsorption on Cu^0 was accompanied by formation of a cyclohexanol alcoholate species and a phenolate species. The existence of the two adsorbed species on Cu^0 explains the low selectivity of catalysts with this active site. In the case of dehydrogenation on Cu^+ copper the kinetics suggests that the reaction proceeds by abstraction of the hydroxyl hydrogen from adsorbed cyclohexanol and formation of the cyclohexanol alcoholate of Cu^+. Hydroxyl hydrogen abstraction was considered to be the rate-determining (rds) step of the reaction. For dehydrogenation of cyclohexanol on Cu^0, the IR and kinetic data were consistent with a dissociative adsorption of cyclohexanol and formation of cyclohexanol alcoholate of Cu^0. The removal of the second nonhydroxyl hydrogen was hypothesized to be the rate-determining step of reaction on Cu^0. The proposed kinetic models for dehydrogenation on the catalysts with Cu^+ and Cu^0 sites give a satisfactory fit to the reaction rate data and provide physically meaningful values for enthalpies and entropies of cyclohexanol and cyclohexanone adsorption.

Keywords: Cyclohexanol; Cyclohexanone; Dehydrogenation kinetics; Copper catalysts; Monovalent and zero-valent copper sites

1. Introduction

The present article is a continuation of our previous study [1] in which we characterized Cu–Mg, Cu–Zn, and Cu–Zn–Al dehydrogenation catalysts by X-ray diffraction, X-ray photoelectron spectroscopy, IR spectroscopy of chemisorbed carbon monoxide, and kinetic methods. This work showed that two types of sites, Cu^0 and Cu^+, are active sites in the dehydrogenation reaction of cyclohexanol to cyclohexanone by these catalysts. Monovalent copper was found to be significantly more active than its zero-valent counterpart. Moreover, the Cu^+ catalysts were shown to be highly selective to cyclohexanone as opposed to the phenol, which is one of the major by-products in the dehydrogenation process. Meanwhile, the Cu^0 catalysts were found to have relatively low selectivity to the ketone, especially at high temperatures and the desirable high cyclohexanol conversions, because of a high rate of phenol formation. Thus, our preceding paper demonstrated a difference between the two kinds of copper-active sites, but did not explain them.

In particular, the reason for the lower activity and selectivity on Cu^0 or the higher activity and selectivity of monovalent copper was not clarified. In order to address these issues, we investigated in detail the mechanisms of adsorption and subsequent dehydrogenation of cyclohexanol on the catalysts with either exclusively Cu^0 or

---

[*] Corresponding author. Current address: Sud-Chemie Inc., 4900 Crittenden Drive, Louisville, KY 40209, USA.

E-mail address: vfridman@sud-chemieinc.com (V.Z. Fridman).

[1] Current address: Department of Chemical Engineering, Massachusetts Institute of Technology, 77 Massachusetts Avenue NE47-591, Cambridge, MA 02139-4307, USA.

0021-9517/$ – see front matter © 2004 Elsevier Inc. All rights reserved.
doi:10.1016/j.jcat.2003.12.016

exclusively Cu^+ sites. This paper is a report of our findings.

Since the cyclohexanol dehydrogenation reaction to cyclohexanone is very important in the caprolactam manufacturing process, the kinetics and mechanism of this reaction on different catalysts have been studied extensively. Specifically, cyclohexanol dehydrogenation on precious metal catalysts [2–4] has received much attention. Takagi et al. [2], for instance, showed that only the hydroxyl hydrogen was replaced based on their radioisotope studies of the dehydrogenation over noble metals. For Pt catalysts, these authors also concluded that cyclohexanol dehydrogenation on Pt proceed via an "enolic" mechanism. Manninger et al. [3] suggested that the cyclohexanol dehydrogenation on Pt might involve a π-allylic surface species intermediate in its structure between the enol and the ketone. This surface species would allow the ring to stay nearly parallel to the catalyst surface and may either desorb as cyclohexanone or stay adsorbed as a phenol. Szilagyi et al. [4] have studied the adsorption of cyclohexanol and cyclohexanone on a Pt/SiO_2 catalyst by IR spectroscopy. They reported *that* dehydrogenation of cyclohexanol to cyclohexanone occurs to a nonnegligible extent even at room temperature and suggest that adsorbed cyclohexanol is bound to the surface by the oxygen atom. In the same paper, the authors conclude that the adsorbed cyclohexanol forms an adsorbed enolic species on the surface Pt/SiO_2.

Surprisingly, although copper has long been the main component of the commercial catalyst for cyclohexanol dehydrogenation, very few fundamental kinetic studies exist in the open literature [5,6]. Medvedeva et al. [5,6] have studied cyclohexanol dehydrogenation on Cu–Mg catalysts by kinetic and deuterium exchange methods. It should be noted that the composition, the preparation, and the reduction conditions of the Cu–Mg catalyst of [5,6] are very similar to those in our work [1]. Based on our results, we believe that the Cu–Mg catalyst of [5,6], after reduction by hydrogen, had only Cu^0-active sites. Therefore, these papers provide data for cyclohexanol dehydrogenation on Cu^0.The most relevant conclusions of [5,6] regarding the cyclohexanol dehydrogenation mechanism are: (i) molecular cyclohexanol adsorption on the Cu–Mg catalyst is the first step of the reaction; (ii) the rate-determining step is the following slow dissociation of the C–H bond in the β position relative to the carbon atom in the C–O bond; (iii) the final steps are the fast rapture of the α-C–H bond in the cyclohexane ring and the following rapid migration of the hydroxylic hydrogen to the β position. Unfortunately [5,6] did not provide direct evidence (e.g., IR data) of the suggested mechanism of nondissociative cyclohexanol adsorption and subsequent abstraction of the hydrogen in the C–H bond. Moreover, according to these reports, removal of the α-hydrogen cannot be the rate-determining step of the reaction in the whole range of temperatures. The authors made this conclusion based on experimental data showing that the rate of α-hydrogen–deuterium exchange was much higher than the cyclohexanol dehydrogenation rate at 170 and 210 °C while at 240 °C according to [5] these rates were close to each other and at 270 °C they were equal. The latter observation suggests that the α-hydrogen abstraction still can be considered the rate-determining steps at the higher temperatures. Moreover, the conclusions are inconsistent with a number of reports (e.g., [2–4,7]) showing that alcohol dehydrogenation reactions start from abstraction of the hydroxylic hydrogen.

Thus, there is still a significant uncertainty about the mechanism of cyclohexanol dehydration on Cu^0. Also, to our knowledge, there are no reports in the open literature regarding kinetics and the mechanisms of the cyclohexanol dehydrogenation on Cu^+. Thus, in this paper we aim to provide the missing information by reporting our results from kinetic investigation and IR spectroscopy of cyclohexanol adsorption and dehydrogenation over catalysts with Cu^0 and Cu^+ sites.

2. Experimental

2.1. Catalysts

Two catalysts were used in this study. The Cu–Mg catalyst prepared according to [1], with a copper loading of 52 at.%, was employed to study the kinetics on Cu^0 sites. Cu^+ catalyst was prepared, also according to [1], on Cu–Zn–Al with a copper loading of 15 at.%. For an IR spectroscopy study of cyclohexanol, cyclohexanone, and phenol adsorption, the Cu–Mg catalyst with a copper loading of 52 at.% and MgO were used.

2.2. Kinetic studies

The reaction kinetics on each catalyst were studied in a continuous flow homogeneous reactor in which the catalyst was suspended in a basket vibrating along the direction of the flow and thus acting as an impeller. We studied the influence of the frequency and amplitude of the catalyst basket vibration on the rate of the cyclohexanol dehydrogenation at 280 °C, where the gradients in temperature and concentration of the reactants and products were expected to be the largest. The vibration frequency and amplitude were chosen so that a further increase in either did not increase the reaction rate (4 Hz and 12 mm, respectively). The kinetic studies were conducted at flow rates in the range of 0.5–4.0 h^{-1} and at temperatures of 220, 250, and 280 °C. In order to eliminate the internal diffusion limitations, we studied the dependence of the reaction rate on the catalyst particle size at 280 °C and found that particle size did not influence the reaction rate for particle diameters below 1 mm. Thus, the catalysts with particles 0.25–0.5 mm in size were used for the kinetic studies.

Cyclohexanol (99.5%) was pumped by a syringe pump into a combined mixer and preheater device where it was vaporized, mixed with helium, and heated to 200 °C. The kinetic studies were carried out at atmospheric pressure and constant initial partial pressure of cyclohexanol equal to 0.82 atm. The partial pressure of He was 0.18 atm. The experiments, in which hydrogen or cyclohexanone was used instead of helium in order to assess the effect of these compounds on the reaction kinetics, were conducted. In these experiments, the initial partial pressure cyclohexanone or hydrogen was also 0.18 atm.

For the kinetic studies, 5 g of catalyst in each experiment was applied. The catalyst samples were reduced by a mixture of 3% of H_2 in N_2 at 250 °C for 16 h before they were used for the reaction. After the reduction, the catalysts were run for 2 h under the appropriate process conditions to allow the reaction to achieve a steady state. To check for catalyst deactivation, each catalyst was tested for about 170 h at 280 °C at a cyclohexanol flow rate of 1 h^{-1}. No changes in catalyst activity in this period of time were observed. During the experiments, 30 min were allowed for equilibration after each change of the process conditions and three measurements were performed under each set of conditions. The average of these three values was used for all subsequent calculations.

The cyclohexanol conversion in the Cu–Zn–Al studies was 7.5–84% and on Cu–Mg catalyst 8–79%. In the Cu–Zn–Al experiments, only trace amounts of cyclohexene and no phenol were observed in the dehydrogenation products. Thus, the selectivity of the catalyst at 220 and 250 °C was close to 100%, and at 280 °C the minimum selectivity was 99.5%. In the Cu–Mg experiments, at 280 °C, trace amounts of cyclohexene and small amounts of the phenol were observed (maximum 0.9%) in the product stream, with the minimum observed selectivity of the catalyst at 98.7%.

2.3. IR spectroscopy

IR spectra of adsorbed cyclohexanol and cyclohexanone were recorded in a temperature range from 25 to 300 °C. A Carl-Zeiss UR-20 infrared spectrometer and FTIR spectrometer Bruker FTS-110 were used to obtain the spectra. The first IR spectrometer was modified for taking IR spectra directly at a high temperature without distortion caused by reverse emission [8]. IR spectra of adsorbed carbon monoxide were used to determine the oxidation state of the copper sites on the catalysts as explained in [1]. The catalysts were pressed into self-supporting thin wafers with transmittance of no less then 20% and placed into a special cell where they were exposed to a gaseous mixture of various compositions at different temperatures. The recorded spectra were compensated for the gas-phase absorption. The details of this method (preparation of the pellets, the cell, the vacuum line procedure for pretreatment of the catalyst sample before adsorption, and conditions of adsorption) are described elsewhere [8,9].

3. Results

3.1. Reaction kinetics

3.1.1. Cyclohexanol dehydrogenation on monovalent copper

The kinetics of cyclohexanol dehydrogenation on Cu^+ was studied using a Cu–Zn–Al catalyst with a Cu loading of 15 at.%. The copper oxidation state on the surface of this catalyst was determined by IR spectroscopy of adsorbed CO as described in Ref. [1]. In the same work, copper was shown to form a solid solution of copper oxide in Zn–Al when Cu loading did not exceed 15 at.%. According to [10, 11] the ZnO lattice surrounding the copper inhibits complete copper reduction under reductive conditions and stabilizes the monovalent form of copper [10,11]. This finding was supported by IR spectroscopy data presented in [1], demonstrating that the IR spectrum of the catalyst after reduction by hydrogen and adsorption of CO displayed only one peak (at 2120 cm^{-1}). This peak did not disappear after evacuation at temperatures as high as 150 °C. Based on the position of this peak and the strength of the Cu–CO complex, it was concluded [1,9,12] that after reduction by a hydrogen-containing gas at 250 °C, a Cu–Zn–Al catalyst had only Cu^+ sites.

To examine the contribution of the support to the total activity of the Cu–Zn–Al catalyst, a $ZnO–Al_2O_3$ system with 15 at.% of Al prepared according to [1] was tested at 250 and 280 °C in the whole range of flow rates used in the kinetic studies. No cyclohexanol conversion was observed at 250 °C and the maximum observed cyclohexanol conversion on Zn–Al sample was 3.4 at.% 280 °C. This value was taken into account to calculate the reaction rate attributed to Cu^+.

The results of the kinetic experiments on the Cu–Zn–Al catalyst (Fig. 1) indicate that the relationship between the cyclohexanol dehydrogenation rate and the partial pressure of cyclohexanol is unaffected by the catalyst surface area coverage. To examine the impact of the reaction products on the reaction rate, hydrogen and cyclohexanone were added to cyclohexanol instead of helium. The cyclohexanol–H_2 and cyclohexanol–cyclohexanone mixtures were tested at 250 °C. The initial partial pressures of the He, H_2, and cyclohexanone were 0.18 atm in all experiments. The experiments indicated that hydrogen does not inhibit cyclohexanol dehydrogenation (Fig. 1, b and d), while the cyclohexanone reduced the reaction rate significantly (Figs. 1, b and e).

Cyclohexanone hydrogenation to cyclohexanol by hydrogen in an equimolar mix of the two reactants (the expected composition of the dehydrogenation products) was studied at 220 and 250 °C. Cyclohexanone flow rates in the range 0.5–4 h^{-1} were used. No conversion of cyclohexanone into cyclohexanol on a Cu–Zn–Al catalyst was observed.

3.1.2. Cyclohexanol dehydrogenation on Cu^0

The rates of cyclohexanol dehydrogenation on Cu^0 were measured on the Cu–Mg catalyst with copper loading of

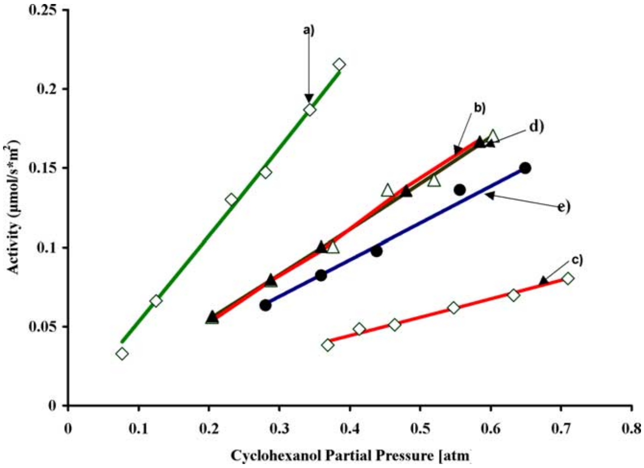

Fig. 1. The rate of the cyclohexanol dehydrogenation to cyclohexanone on the Cu–Zn–Al catalyst with monovalent copper sites as a function of the partial cyclohexanol pressure: Solid lines denote the best fits of Eq. (14) to the data; the symbols are experimental points. (a) 280 °C (cyclohexanol–He); (b) 250 °C (cyclohexanol–He); (c) 220 °C (cyclohexanol–He); (d) 250 °C (cyclohexanol–H_2); (e) 250 °C (cyclohexanol–cyclohexanone).

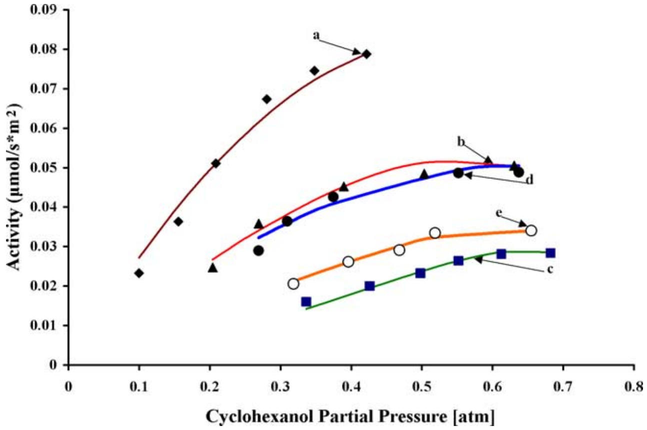

Fig. 2. The rate of the reaction of the cyclohexanol dehydrogenation to cyclohexanone on the Cu–Mg catalyst with zero-valent copper sites as a function of partial pressure of alcohol: Solid lines denote the best fits of Eq. (28). Symbols are experimental points. (a) 280 °C (cyclohexanol–He); (b) 250 °C (cyclohexanol–He); (c) 220 °C (cyclohexanol–He); (d) 250 °C (cyclohexanol–H_2); (e) 250 °C (cyclohexanol–cyclohexanone).

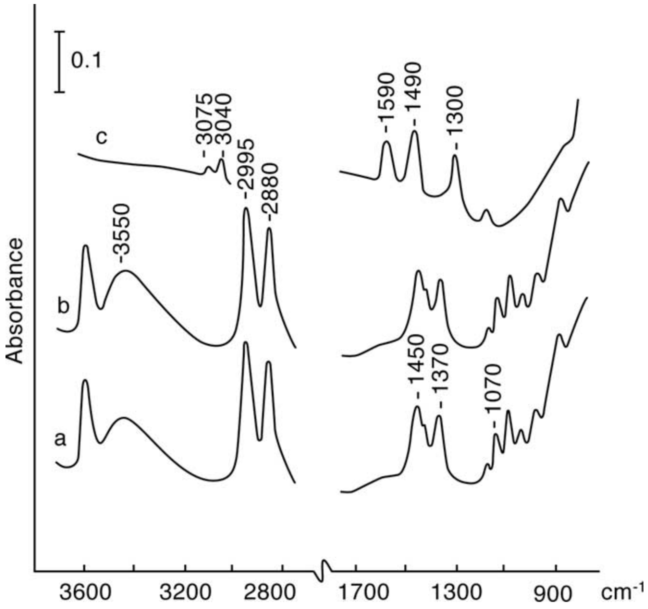

Fig. 3. IR spectra of adsorbed cyclohexanol at 25 °C (a), at 250 °C (b), and phenol at 25 °C (c) on the surface of the MgO.

52 at.%. This catalyst has been evaluated in detail in [1]. In particular, the IR spectrum of the catalyst sample that had been reduced by exposure to hydrogen-containing gas at 250 °C for 16 h, and subsequently treated with CO, showed only one peak—at 2080 cm^{-1}. This absorbance band completely disappeared after evacuation at 25 °C. Based on literature data [9,12], the position of the band, and strength of the Cu–CO complex, it was concluded that only Cu^0-active sites were present on the catalyst surface. To examine the contribution of the support to the total activity of Cu–Mg catalyst, the magnesium oxide prepared according to [1] was tested at 250 and 280 °C in whole range of flow rates. No cyclohexanol conversion was observed at 250 °C and a conversion of 0.9% was observed at 280 °C. This value was taken into account for the calculation of the reaction rates at 280 °C.

The results of the kinetic study (Fig. 2) show that the cyclohexanol dehydrogenation rate increases almost linearly with the partial pressure of cyclohexanol for low surface area coverage (Fig. 2, a, b, and c). The growth of the reaction rate with partial pressure slows down when the cyclohexanol partial pressure reaches about 0.3 atm. This type of behavior is usually indicative of strong adsorption of the reactant.

As in the case with the Cu–Zn–Al system, the effect of the reaction products on the dehydrogenation rate was studied. Helium in the reactant mixture was replaced by H_2 or cyclohexanone at 250 °C. H_2 did not have any discernible negative impact on the rate of cyclohexanol dehydrogenation (Fig. 2, b and d). Cyclohexanone, however, decreased the reaction rate significantly (Fig. 2, b and e).

To determine the effect of the reverse reaction, the cyclohexanone hydrogenation was studied in an equimolar mix of cyclohexanone and hydrogen at 220 and 250 °C. The flow rate range was 0.5–4 h^{-1}. No conversion of cyclohexanone to cyclohexanol was observed on the Cu–Mg catalyst under these conditions.

3.2. IR spectroscopy data: Adsorption of cyclohexanol, cyclohexanone, and phenol

3.2.1. Cyclohexanol and phenol adsorption on MgO

The Cu–Mg catalyst was used to study the cyclohexanol, cyclohexanone, and phenol adsorption on Cu^+- and Cu^0-active sites. In order to account for the effects of the support, it was important to study the adsorption of these compounds on pure MgO. The IR spectrum of cyclohexanol adsorbed on the MgO at 25 °C (Fig. 3, a) displayed a series of peaks that are mainly the same as those of pure cyclohexanol [13,14]. The appearance of the absorption bands that exist in the IR spectrum of the pure cyclohexanol in the IR spectrum of the cyclohexanol adsorbed on MgO, including the wide absorption peak at 3550 cm^{-1} assigned to the stretching mode of hydroxyl groups, indicates that one of the adsorption species is nondissociative. This IR spectrum also shows an absorption band at 3750 cm^{-1} (Fig. 3, a) that, according to [9], should be assigned to the stretching mode of the surface hydroxyl groups on MgO. The intensity and shape of the absorption band at 3750 cm^{-1} before and after cyclohexanol adsorption on MgO (the spectrum of pure MgO is not shown) were the same. This indicated that these OH groups do not participate in the cyclohexanol adsorption on the surface of MgO (Fig. 3, a and b). The absorption peaks at 1090–1100, 1130, and 1150 cm^{-1} were assigned to the stretching modes of a C–O bond in, for example, an alcoholate species [9] that is formed with the participation of magnesium oxide sites. The formation of the alcoholate species after alcohol adsorption is usually accompanied by a shift of the C–O bond stretching modes to a higher range [9]. Besides the band at 1090 cm^{-1} that is close to the position of the stretching band of the C–O bond in pure cyclohexanol, this spectrum had the bands at 1130 and 1150 cm^{-1} that would appear as a result of the alcoholate species formation. Thus, based on the IR data, it was concluded that, as result of the adsorption, cyclohexanol exists on the surface of MgO as both a molecular cyclohexanol and the alcoholate surface species.

Increasing the temperature to 250 °C led to the appearance of the small peak at 1620 cm^{-1} and increase of the absorbance intensity at 3550 cm^{-1} (Fig. 3, b). This is the expected effect of the water adsorption formed in the alcohol dehydration reaction. The cyclohexanol adsorption on the surface of MgO and a subsequent increase in temperature have not generated cyclohexanone or phenol, showing that MgO is not active in these reactions under the given conditions.

3.2.2. *Phenol adsorption*

Besides cyclohexanol, phenol adsorption on MgO was studied. The spectrum of phenol adsorbed on MgO at 20 °C (Fig. 3, c) shows peaks at 1170, 1300, 1490, and 1590 cm^{-1}. These peaks are in good agreement with the spectrum of pure phenol [13,14] and phenol on MgO and CuO [15].

3.2.3. *Cyclohexanol adsorption on monovalent copper site*

The Cu–Mg catalyst with a copper loading of 52 at.% was used to study cyclohexanol adsorption on Cu^+ sites. The Cu–Mg catalyst was reduced by CO at 100 °C with a subsequent evacuation of CO at 250 °C to form the partly oxidized copper sites on the surface. The spectrum of CO adsorbed on the resulting catalyst (spectrum is not shown) displayed a peak at 2120 cm^{-1} that persisted after evacuation at 150 °C. This indicates that the copper on the surface of Cu–Mg catalyst has indeed been reduced by the above-noted treatment to Cu^+ [1,9,12]. The subsequent cyclohexanol adsorption on this catalyst at 25 °C led to the appearance of a series of peaks characteristic of pure cyclohexanol [13,14] (the peaks at 890, 970, 1025, 1070, 1360, 1450, 2880, and 2995 cm^{-1}; Fig. 4, b).

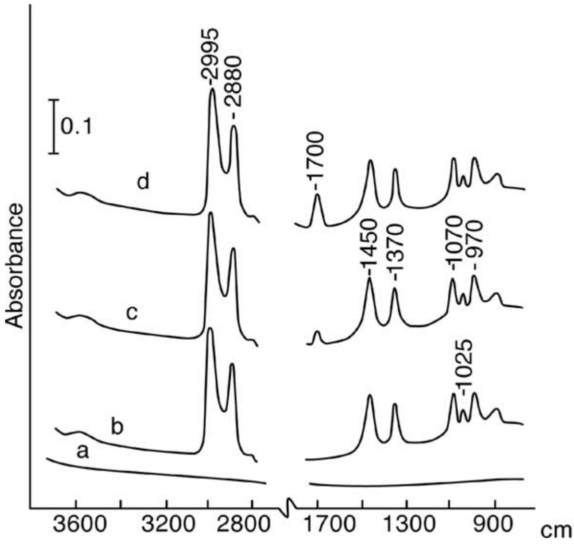

Fig. 4. IR spectra of cyclohexanol on the surface of monovalent copper (Cu–Mg catalyst 52% of copper); (a) initial catalyst after reduction in CO at 100 °C and vacuum treatment at 250 °C for 2 h; (b) sample (a) after adsorption of cyclohexanol at 25 °C; (c) sample (b) after vacuum treatment at 25 °C; (d) sample (c) after vacuum treatment at 100 °C.

Unlike a typical spectrum of the alcohol [13], this spectrum displayed a weak and narrow peak around 3550 cm^{-1} (Fig. 4, b and c). Usually the O–H stretching peak at 3500–3600 cm^{-1} has a maximum intensity comparable to that of other major peaks of the alcohol [13,14]. There are two possible scenarios that might explain the appearance of this low intensity peak at 3550 cm^{-1}. The first is that the dehydrogenation reaction starts with a molecular adsorption of cyclohexanol on Cu^+ and proceeds with the abstraction of the hydroxyl hydrogen and formation of the strongly bonded alcoholate. In this case, the IR spectrum would include contributions both from cyclohexanol and the alcoholate. However, molecular adsorption of cyclohexanol is likely to be weak, and therefore, the intensity of the characteristic O–H stretching peak at 3550 cm^{-1} (Fig. 4, b and c) in the composite spectrum would be relatively small. The appearance of the peak can also be explained by assuming a dissociative adsorption of cyclohexanol on Cu^+ with formation of cyclohexanol alcoholate. The cyclohexanol alcoholate allylic hydrogens interact with a nearby oxygen atom of the Cu^+–ZnO lattice. This situation is illustrated in Fig. 6. The stretching of these isolated O–H groups would then lead to the appearance of the peak at 3550 cm^{-1}. It should be noted that this type of interaction could occur in both suggested scenarios. A similar assumption in the case of alcohol adsorption has been made in [16].

In the present study, when the Cu–Mg catalyst with cyclohexanol adsorbed on the Cu^+ was evacuated at 25 °C, a weak absorption peak at 1700 cm^{-1} (Fig. 4, c) appeared in the IR spectrum. The peak was assigned to a ν C=O bond in cyclohexanone [13,14]. Increasing the temperature to 100 °C led to an increase in the intensity of this peak (Fig. 4, d).

3.2.4. Cyclohexanol and cyclohexanone adsorption on Cu^0

Prior to the cyclohexanol adsorption, the Cu–Mg catalyst was reduced by the hydrogen-containing gas at 250 °C to form the metallic state of copper on its surface. The oxidation state of copper after the catalyst reduction was evaluated by IR spectroscopy of adsorbed CO. The IR spectrum of adsorbed CO showed only one peak, at 2080 cm^{-1}, that disappeared after catalyst evacuation at 25 °C (the spectrum is not shown in this paper but it is similar to that presented in [1]). The position of the peak and the stability of the Cu–CO complex confirmed that there were only Cu^0 sites on the surface of the Cu–Mg catalyst after its reduction by hydrogen [1,9,12]. The IR spectrum of the reduced Cu–Mg catalyst, after an exposure of cyclohexanol at 25 °C, did not display any absorption bands (Fig. 5, b). After cyclohexanol adsorption on the Cu–Mg catalyst at 50 °C, the IR spectrum displayed in wavenumbers rangeing between 1000 and 1800 cm^{-1} three bands at 1300, 1490, and 1590 cm^{-1} (Fig. 5, c) that correspond closely to the spectrum of the phenolate-like species [15]. According to [13,14], the peak at 1300 cm^{-1} can be attributed to the stretching of the C–O bond in the phenolate. The bands at 1490 and 1590 cm^{-1} can be assigned to the symmetric and asymmetric stretching of carbon–carbon bonds in an aromatic ring [13,14]. Furthermore, this spectrum (Fig. 5, c) has strong peaks at 2880 and 2995 cm^{-1} that correspond closely to the peaks in the spectrum of pure cyclohexanol [13] and cyclohexanol adsorbed on MgO (Fig. 3, a and b). These bands can be assigned to the stretching of the C–H bonds in the cyclohexane ring [13,14], thus indicating the presence of cyclohexane rings in the species formed after the adsorption of cyclohexanol on Cu^0.

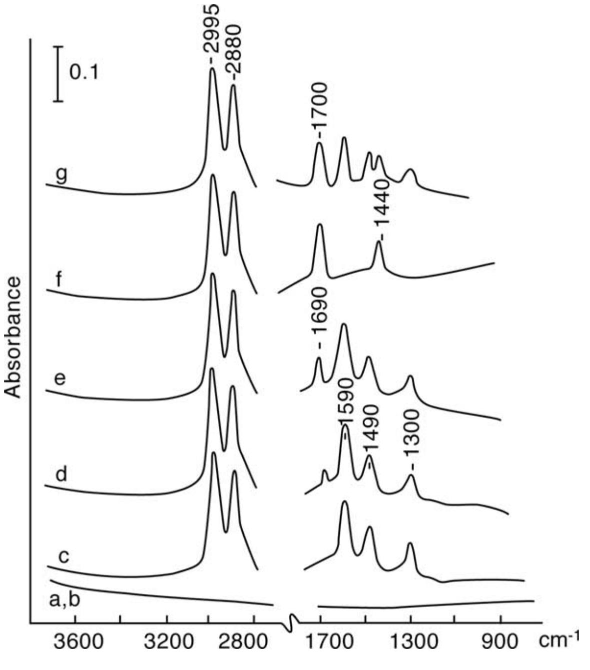

Fig. 5. IR spectra of cyclohexanol and cyclohexanone adsorbed on the surface of zero-valent copper (Cu–Mg catalyst): (a) initial Cu–Mg catalyst after reduction in H_2 at 250 °C and vacuum treatment at the same temperature for 1 h; (b) sample (a) after adsorption of cyclohexanol at 25 °C; (c) sample (a) after adsorption of cyclohexanol at 50 °C; (d) sample (c) after heating up to 200 °C; (e) sample (d) after heating up to 250 °C; (f) sample (a) after adsorption cyclohexanone at 25 °C; (g) sample a after adsorption of cyclohexanone at 25 °C and heating up to 200 °C.

Surprisingly, the spectrum of cyclohexanol adsorbed on Cu^0 did not have the peak at 1070–1100 cm^{-1} that is present in the spectra of pure cyclohexanol or alcoholate, and is assigned to the stretching modes of the C–O bond of cyclohexanol (Fig. 5, c) [13,14]. The possible reason for the absence of this peak might be the orientation of adsorbed cyclohexanol relative to the surface copper surface. According to the “metal-surface selection rule” of Pearce and Sheppard [17], only those vibrations with the oscillating dipole moment perpendicular to the metal surface will be infrared active. Because the copper clusters are large (approximately 12 nm in diameter, [1]) relative to the size of the cyclohexanol molecule, they can be considered approximately flat in the present context. Thus, we believe that there is the C–O bond in the cyclohexanol species adsorbed on Cu^0, but it is infrared inactive simply because it is parallel to a cluster surface.

As indicated earlier, according to Szilagyi et al. [4], the cyclohexanol transformation into cyclohexanone on Pt occurs via a π-allylic type (O=C=C-type compound, usually referred to as an enol, intermediate in its nature between an alcohol and a ketone). We considered the possibility of the enol-type species formation in our study for cyclohexanol dehydrogenation on zero-valent copper. However, we did not find enough evidence to prove the existence of the enol-type of species after cyclohexanol adsorption on the zero-valent copper sites. As follows from the literature IR spectroscopy studies of ketone adsorption on the oxides [18–21], a formation of the enol-type compounds is usually accompanied by the appearance of two additional absorption peaks in the range of 1350–1450 and 1510–1570 cm^{-1} in the IR spectrum the adsorbed species. The IR spectrum of adsorbed cyclohexanol on zero-valent copper sites did not have absorption bands that usually exist in the IR spectrum of enol-like species (Fig. 5, c). There are examples in the literature [22,23] where authors studied acetone adsorption by means of IRS on single crystal of Pt and Pd, and also did not find any indication of the enol-type species formation.

Another feature of the IR spectrum of cyclohexanol adsorbed on Cu^0 is that this spectrum (Fig. 5, c) does not have an O–H stretching peak at 3500–3550 cm^{-1} characteristic of molecular cyclohexanol [13,14]. The absence of this peak at 50 °C indicates that adsorption is accompanied by a rupture of the O–H bond and formation an alcoholate species on the copper surface. The IR spectrum also showed peaks assigned to aromatic and cycloalkane compounds, leading

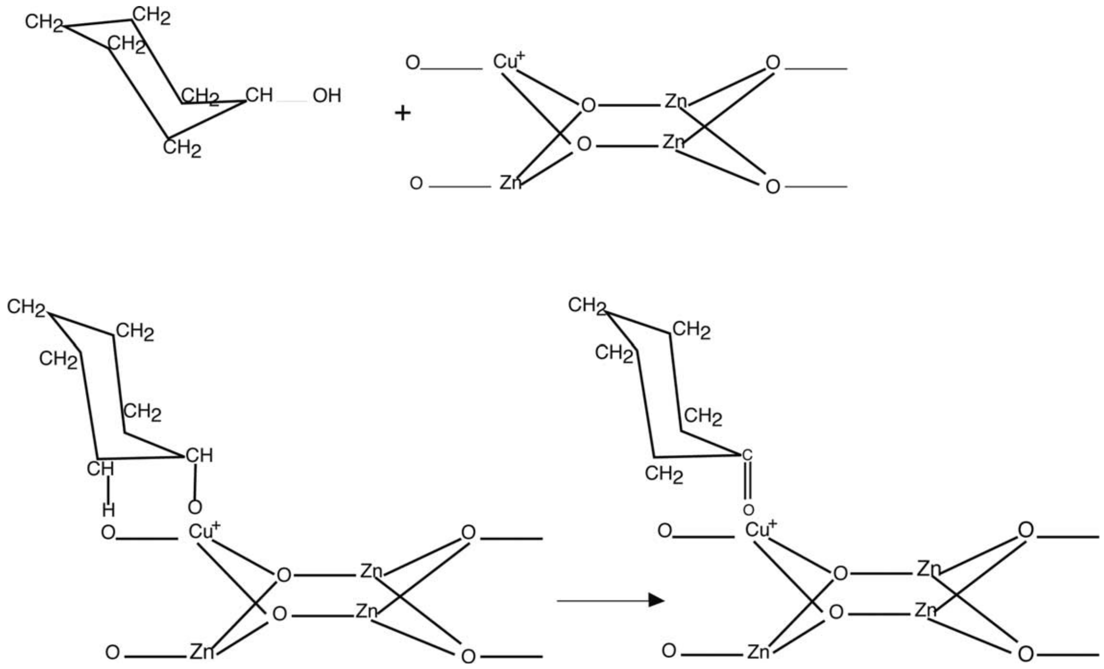

Fig. 6. Schematic of cyclohexanol adsorption on the surface of monovalent copper.

to the conclusion that the adsorption of cyclohexanol on Cu^0 at 50 °C is accompanied by the simultaneous formation of strongly adsorbed phenolate-like and cyclohexanol alcoholate-like species, neither of which contains a hydroxyl group.

The subsequent heating of adsorbed cyclohexanol on the surface of the Cu–Mg catalyst from 50 to 150 °C resulted in the IR spectrum no change (spectra at 100 and 150 °C are not shown). The absorption peak at 1690 cm^{-1} was observed only when the catalyst temperature achieved 200 °C (Fig. 5, d). Increasing the temperature to 250 °C intensified the peak at 1690 cm^{-1} (Fig. 5, d and e). This absorption band was attributed to the stretching of the ν C=O in cyclohexanone [13,14], which was produced from the adsorbed cyclohexanol. It should be noted that in the case of cyclohexanol alcoholate of Cu^+, the peak at 1700 cm^{-1} was observed after evacuation of the catalyst at a temperature as low as 25 °C (Fig. 4, c). This observation further supports the conclusion that Cu^+-active sites are much more active than Cu^0 sites [1].

3.2.5. *Cyclohexanone adsorption on Cu^0*

The spectra of cyclohexanone adsorbed on Cu^0 sites at 25 °C (Fig. 5, f) were similar to the spectrum of pure cyclohexanone [13,14], with one of the most prominent peaks at 1700 cm^{-1} (ν C=O). The subsequent heating of adsorbed cyclohexanone to 200 °C led to a decrease in the intensity of the peak at 1700 cm^{-1} and the appearance of the peaks at 1590, 1490, and 1290 cm^{-1} (Fig. 5, g) that are attributed to the phenolate species [13,14]. This result suggests that cyclohexanone, like cyclohexanol, can be converted to phenol by the Cu^0 sites of the catalyst.

4. Discussion

4.1. *Mechanism of the cyclohexanol dehydrogenation on the Cu^+*

The mechanism of cyclohexanol dehydrogenation on monovalent copper has, to our knowledge, never been investigated before. However, the adsorption of cyclohexanol on Cu^+ sites can be compared with the more general alcohol adsorption on oxide catalysts extensively studied in Refs. [9,24–26]. It is shown in [9] that the alcohol usually forms three types of adsorbed species on the catalyst surface: (1) molecularly adsorbed alcohol held at the surface by the hydrogen bonds of CH_2, CH_3, or OH and the surface; (2) coordinately bound alcohol; and (3) alcoholate. The alcoholate species are the most strongly adsorbed [9]. As explained above, the IR data suggest two scenarios for the mechanism of cyclohexanol adsorption on Cu^+. There is a possibility of the dissociative adsorption of cyclohexanol on Cu^+, where the allylic hydrogens interact with the oxygen atoms of the Cu^+–ZnO lattice as indicated in Fig. 6. The second scenario starts with nondissociative adsorption of cyclohexanol on Cu^+ and proceeds with the abstraction of the hydroxylic hydrogen and formation of the cyclohexanol alcoholate of Cu^+. The hydrogens of the CH_2 group of the cyclohexanol alcoholate may still interact with a surface oxygen atom.

In both scenarios, the intermediate for cyclohexanone formation is the adsorbed alcoholate species. It should be pointed out that this species is very reactive. Fig. 4 shows that even after evacuation of cyclohexanol adsorbed on Cu^+ at 25 °C, the IR spectrum has a peak at 1700 cm^{-1} indicating the transformation of cyclohexanol alcoholate into cyclohexanone. This observation suggests that, very likely, the second hydrogen removal from cyclohexanol alcoholate of Cu^+ is not the rate-determining step.

The dependence of the reaction rate on the partial pressure of cyclohexanol and cyclohexanone (Fig. 1) can provide some further clues about the reaction mechanism. First, cyclohexanol does not appear to have any inhibiting influence on the reaction rate in the entire range of pressures. This suggests that cyclohexanol adsorption is weak. The second clue is that there appears to be a strong competitive adsorption of cyclohexanone, as indicated by the decrease in the reaction rate when helium was replaced by the ketone (Fig. 1, b and e). Next, we note that hydrogen appears to have no negative impact (Fig. 1, b and d) on the dehydrogenation rate. This is possible only in two cases: (1) there is no reverse hydrogenation reaction (our results show this to be true) and (2) hydrogen adsorption is relatively weak or even negligible in the reaction mechanism. According to the model of Herman and co-workers [10,11], in Cu–Zn catalysts Cu^+ is stabilized as isolated ions surrounded by Zn and oxygen of the solid solution of Cu^+ in the lattice of ZnO. Because the Cu^+ ion is isolated, we believe that hydrogen adsorption on Cu^+ is unlikely. However, it is known that hydrogen can be adsorbed by ZnO [27,28]. Herman and co-workers also considered hydrogen adsorption on ZnO in the context of their study of methanol synthesis [10]. According to their kinetic model, CO is strongly adsorbed on Cu^+ and eventually is hydrogenated by H atoms migrating from the ZnO.

A number of kinetic models were considered for dehydrogenation of cyclohexanol on Cu^+. In brief they were:

1. Dissociative cyclohexanol adsorption as a first step of a reaction where cyclohexanol interacts with Cu^+ and hydrogen adsorption occurs on an X adsorption site other than Cu^+.
2. Dissociative cyclohexanol adsorption as a first step and hydrogen recombination in the gas phase.
3. Molecular adsorption of cyclohexanol with subsequent abstraction of the hydroxylic hydrogen as a second step, with hydrogen adsorption on an X site other than Cu^+.
4. Molecular adsorption of cyclohexanol with subsequent rupture of the O–H bond and hydrogen recombination in the gas phase.

In each model, one surface step of the reaction sequences, such as abstraction of the hydroxyl hydrogen or of the α-hydrogen, was considered as irreversible and rate determining. This assumption is motivated by the fact that no hydrogenation of cyclohexanone by H_2 on Cu–Zn–Al catalyst was observed experimentally. All other steps were assumed to be in quasi-equilibrium. Also, H_2 was assumed to either adsorb onto some site X other than Cu^+ or to not adsorb at all. In the latter case, H_2 was assumed to form in a gas-phase reaction of two hydrogen atoms. This treatment still allows the possibility of hydrogen adsorption on ZnO, but ensures that H_2 partial pressure does not directly influence the dehydrogenation rate.

Rate parameters for each model were determined by fitting it to the data using a nonlinear least-squares algorithm. The model discrimination was done based on the fit of experimental results to calculated rate values. The best match between experimental data and calculated results was obtained for the following mechanisms: (1) molecular adsorption of cyclohexanol on Cu^+; (2) irreversible, rate-determining abstraction of the hydroxylic hydrogen and hydrogen atom migration into the gas phase; (3) removal of the second hydrogen produces cyclohexanone; (4) cyclohexanone desorption; and (5) hydrogen recombination in gas phase. Equations (1)–(5) summarize this mechanism:

$$Cu^+ + C_6H_{11}OH(\text{gas}) \leftarrow K_{CLL} \rightarrow C_6H_{11}OHCu^+, \tag{1}$$

$$C_6H_{11}OHCu^+ — K_2 \rightarrow C_6H_{11}OCu^+ + H(\text{gas}), \tag{2}$$

$$Cu^+C_6H_{11}O \leftarrow 1/K_3 \rightarrow Cu^+C_6H_{10}O + H(\text{gas}), \tag{3}$$

$$Cu^+C_6H_{10}O \leftarrow 1/K_{CLN} \rightarrow Cu^+ + C_6H_{10}O(\text{gas}), \tag{4}$$

$$2H(\text{gas}) \leftarrow 1/K_4 \rightarrow H_2(\text{gas}). \tag{5}$$

Now the rate equation for this mechanism can be derived. If removal of the first hydrogen atom in the O–H bond is assumed to be irreversible and rate determining, the rate of cyclohexanone formation, R_{CLN}, is given by

$$R_{CLN} = LK_2\theta_{CLL}, \tag{6}$$

where L is the total number of active sites, K_2 is forward rate constant of step (2), and θ_{CLL} is the fractional coverage of the catalyst surface by cyclohexanol. From the definition of the fractional coverage, the following balance equation follows,

$$1 = \theta\text{v} + \theta_{CLL} + \theta_{CLA} + \theta_{CLN}, \tag{7}$$

where θv is fraction of vacant active sites, θ_{CLL} is fractional coverage of cyclohexanol, θ_{CLA} is fractional coverage of cyclohexanol alcoholate, and θ_{CLN} is fractional coverage of cyclohexanone. Furthermore, the quasi-equilibrium assumption for the adsorption of cyclohexanol and cyclohexanone on Cu^+ can be expressed as

$$\theta_{CLL} = K_{CLL}P_{CLL}\theta\text{v}, \tag{8}$$

$$\theta_{CLN} = K_{CLN}P_{CLN}\theta\text{v}, \tag{9}$$

$$\theta_{CLA} = K_3K_4^{1/2}K_{CLN}P_{CLN}\theta\text{v}P_{H_2}^{1/2}. \tag{10}$$

These equations can now be substituted into Eq. (7) to yield

$$\begin{aligned}1 = \theta\text{v} &+ K_{CLL}P_{CLL}\theta\text{v} + K_{CLN}P_{CLN}\theta\text{v}\\ &+ K_3K_4^{1/2}K_{CLN}P_{CLN}\theta\text{v}P_{H_2}^{1/2},\end{aligned} \tag{11}$$

$$\begin{aligned}\theta\text{v} = 1/\bigl(1 &+ K_{CLL}P_{CLL} + K_{CLN}P_{CLN}\\ &+ K^*K_{CLN}P_{CLN}P_{H_2}^{1/2}\bigr),\end{aligned} \tag{12}$$

Table 1
Optimized rate parameters in Eqs. (14) and (28)

Temperature (°C)	Optimized rate parameters in Eq. (14) for Cu–Zn–Al catalyst with monovalent copper			
	K (μmol/(s g_{cat})/atm)	K^* ($atm^{-1/2}$)	K_{CLL} (atm^{-1})	K_{CLN} (atm^{-1})
220	0.119	0.034	0.057	0.220
250	0.295	0.057	0.031	0.181
280	0.573	0.081	0.020	0.157
	Optimized rate parameters in Eq. (28) for Cu–Mg catalyst with zero-valent copper			
	K (μmol/(s g_{cat}))	K_{H_2} (atm^{-1})	K_{CLL} (atm^{-1})	K_{CLN} (atm^{-1})
220	0.223	1.121	1.474	5.394
220	0.361	0.432	1.186	2.700
280	0.464	0.179	0.613	1.227

Table 2
Kinetic and thermodynamic parameters for cyclohexanol dehydrogenation

E_{rds} (kcal/mol)	Compound	ΔH^0_{ad} (kcal/mol)	ΔS^0_{ad} (cal/(mol K))	ΔS^0_{gas} (cal/(mol K))
Parameters obtained for Cu–Zn–Al catalyst with monovalent copper sites				
11.5	Cyclohexanol	−6.3	−19.1	85.4[a]
	Cyclohexanone	−6.2	−15.2	76.9[b]
Parameters obtained for Cu–Mg catalyst with zero-valent copper sites				
9.0	Cyclohexanol	−7.5	−14.5	85.4[a]
	Cyclohexanone	−14.2	−25.0	76.9[b]
	H_2	−13.9	−28.7	31.2[b]

[a] [42].
[b] [41].

where K^* is $K_3 K_4^{1/2}$.

Substitution of θ_{CLL} from Eq. (8) into Eq. (6) yields

$$R_{CLN} = L K_2 K_{CLL} P_{CLL} \theta v \tag{13}$$

and the final rate expression is

$$R_{CLN\ on\ Cu^+} = K K_{CLL} P_{CLL} / \big(1 + K_{CLL} P_{CLL} + K_{CLN} P_{CLN} + K^* K_{CLN} P_{CLN} P_{H_2}^{1/2}\big), \tag{14}$$

where $K = L K_2$.

The best fit parameters at the three temperatures are listed in Table 1 and the fits to experimental data are shown in Fig. 1. The activation energy of the second reaction step, enthalpies, and entropies of cyclohexanol and cyclohexanone adsorption obtained from the temperature dependence of the equilibrium adsorption constants are presented in the Table 2. The model appears to fit the data very well (Fig. 1). Moreover, the model is in a good agreement with the experimental observations that cyclohexanol adsorption is relatively weak (kinetic studies) and the removal of the α-hydrogen is a relatively fast step (IR data).

4.2. Mechanism of the cyclohexanol dehydrogenation on Cu^0

Our previous study [1] showed that zero-valent copper sites suffer from low selectivity, producing phenol as a byproduct of cyclohexanol dehydrogenation at high temperatures. The IR data obtained in the present work provide an explanation for this low selectivity. The simultaneous formation of the phenolate species and cyclohexanol alcoholate species as a result of cyclohexanol adsorption allows the formation of both products.

Phenol formation has long been a subject of discussion in studies devoted to cyclohexanol dehydrogenation [29]. There are three known pathways for phenol formation from cyclohexanol: (1) direct dehydrogenation via aromatization of the cyclohexane ring in cyclohexanol; (2) phenol formation from the product cyclohexanone; (3) phenol formation both from cyclohexanol and cyclohexanone [30,31]. We have already presented our conclusions regarding the mechanism of phenol formation on Cu^0 in Ref. [32]. According to [32] and results of the present study, both cyclohexanol and cyclohexanone adsorbed on Cu^0 can form a phenolate species that is an intermediate in the formation of phenol.

The primary question we seek to answer about cyclohexanol dehydrogenation to cyclohexanone on Cu^0 is the character of the cyclohexanol adsorption. There are a many studies in the literature showing that a variety of alcohols form an alcoholate-adsorbed species on a number of different catalysts [33–35]. In a recent paper, Rioux and Vannice [7] presented DRIFT results for the isopropanol adsorption on carbon-supported copper with Cu^0 surface-active sites. The authors observed molecular adsorption of isopropanol and isopropoxide onto Cu^0. The IR spectrum of adsorbed isopropanol reported by the authors does not show the O–H stretching peak at 3663 cm^{-1}, but does display the peak at 1272 cm^{-1} assigned to a δ-(O–H) bending mode of the molecularly adsorbed isopropanol. Both results are in agreement with our findings for cyclohexanol.

As discussed under Experimental of the present paper, this study shows the existence of molecularly adsorbed cyclohexanol and cyclohexanol oxide on MgO (Fig. 3). However, there is no evidence demonstrating the presence of adsorbed molecular cyclohexanol on metallic copper (Fig. 5). At 25 °C, the IR spectrum of the Cu–Mg catalyst after cyclohexanol adsorption on Cu^0 is completely flat (Fig. 5, b). The first sign of cyclohexanol adsorption appears only at 50 °C, when a breakage of the O–H bond facilitates the adsorption by delocalizing the electron density on the carbon atoms of the cyclohexane ring. Thus, we believe that the cyclohexanol adsorption on Cu^0 is a dissociative process in which the C–O bond of the cyclohexanol interacts with metallic copper as indicated in Fig. 7.

As we noted above, the IR spectrum of cyclohexanol adsorbed on Cu^0 indicates that adsorbed species of two types are formed simultaneously. The first type is a phenolate species and the second type is a cyclohexanol alcoholate.

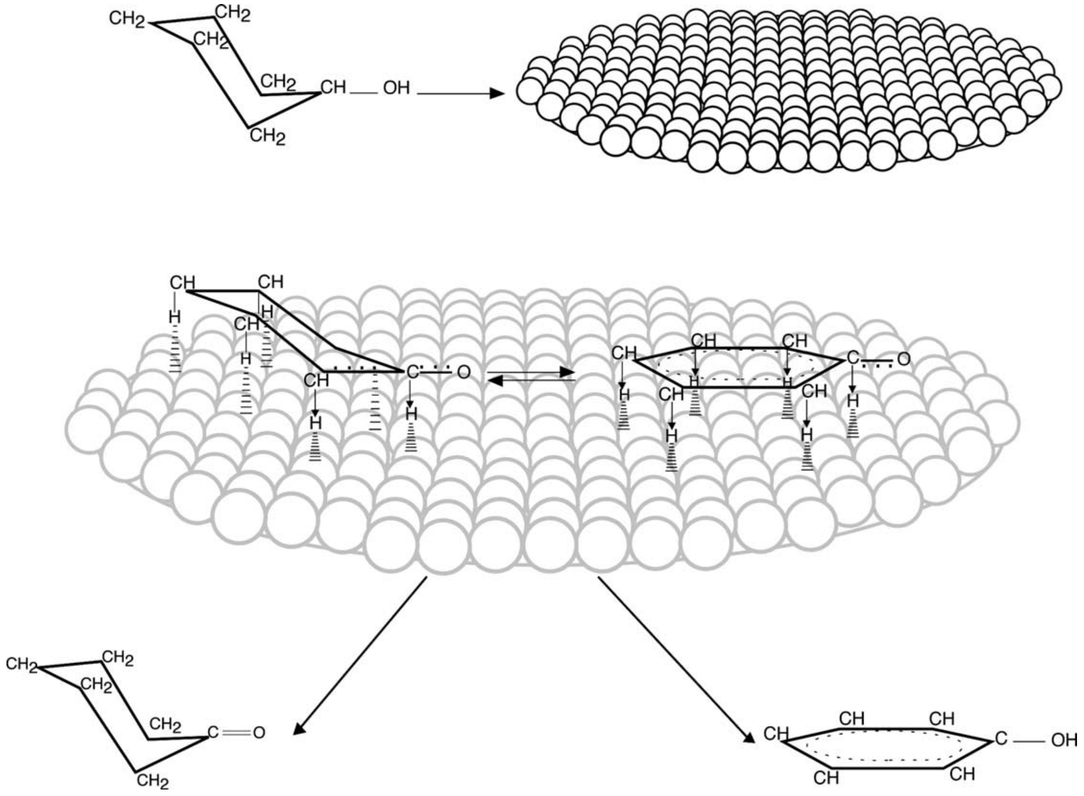

Fig. 7. Schematic of cyclohexanol adsorption on the surface of zero-valent copper.

Most likely, only one type among these species is the intermediate for cyclohexanone formation. Increasing the temperature of the Cu–Mg catalyst with these species on the surface up to 100 and 150 °C did not change the IR spectrum of the catalyst (spectra are not shown in this paper). At 200 °C, a small peak appeared at 1690 cm^{-1} (Fig. 5, d); the intensity of the peak went up by a factor of 3 when the temperature was raised to 250 °C (Fig. 5, e). The appearance of this absorption band is an indication that one of the two adsorbed species has been converted into cyclohexanone. The fact that cyclohexanone appeared on the surface only at a temperature as high as 200 °C indicates that the formation of adsorbed cyclohexanone is a relatively slow step that is likely to be rate determining.

To identify the intermediate for the cyclohexanone formation, the intensity of the absorption peaks assigned to the phenol-like species and to the cyclohexanol alcoholate species was measured before and after the appearance of the C=O peak in IR spectrum (Fig. 5, c and d). Although a phenolate species is not a thermodynamically favorable intermediate for cyclohexanone formation, and therefore is unlikely, both species were considered as possible intermediates. The intensities of the IR absorption peaks at 1300, 1490, 1590 cm^{-1} (the phenolate species) and 2880 and 2995 cm^{-1} (cyclohexanol alcoholate of Cu^0) at 50, 200, and 250 °C are juxtaposed in Fig. 5 (c, d, and e). The comparison reveals that there is no discernible difference in intensity of the peaks among the three IR spectra. The fact that the phenolate peaks (1300, 1490, and 1590 cm^{-1}) are unaffected by temperature suggests that the phenolate species is not involved in the cyclohexanone formation.

The observation that the peaks at 2880 and 2995 cm^{-1} are unchanged is expected. The IR spectra of the adsorbed cyclohexanol and the adsorbed cyclohexanone (Fig. 5, c and f) show the same characteristic peaks in the range of wavenumbers above 2800 cm^{-1}. The conversion of the cyclohexanol alcoholate species into cyclohexanone should not affect IR peaks due to CH_2 groups because these groups are not consumed in the reaction. Although there was no changes in intensity of the absorption peaks at 2880 and 2950 cm^{-1}, the necessity of cyclohexane ring for cyclohexanone formation lead us to conclude that, most likely, the cyclohexanol alcoholate of Cu^0 species is the intermediate for cyclohexanone synthesis on Cu^0.

More supporting information about the reaction mechanism can be extracted from the dependence of the dehydrogenation rate on the partial pressures of cyclohexanol, hydrogen, and cyclohexanone. Fig. 2 shows the inhibiting influence of the cyclohexanol on the reaction rate at the higher partial pressures of cyclohexanol, suggesting that the cyclohexanol adsorption is relatively strong. The decrease in the reaction rate upon the addition of cyclohexanone to the reactant mix (Fig. 2, b and e) indicates that the cyclohexanone adsorption on Cu^0 is strongly competitive. Hydrogen does not appear to have any effect on the reaction rate (Fig. 2, b and d). This observation is consistent with literature data showing weak hydrogen adsorption on metallic copper [7,36–38]. Fig. 7 summarizes our conclusions regarding the dissociative cyclohexanol adsorption on Cu^0 and the two types of adsorbed species.

As in the case of the monovalent copper, a number of kinetic models for the dehydrogenation of cyclohexanol on zero-valent copper were considered in this study. Specifically, the two most important types of models considered were:

1. Dissociative adsorption of cyclohexanol on metallic copper followed by formation of cyclohexanol alcoholate and dissociatively adsorbed hydrogen.
2. Molecular adsorption of cyclohexanol with subsequent abstraction of the hydroxylic hydrogen, followed by the formation of cyclohexanol alcoholate and dissociatively adsorbed hydrogen.

The second model was considered despite the fact that IR spectroscopy data showed no sign of nondissociative adsorption of cyclohexanol.

Since no cyclohexanone hydrogenation on Cu^0 has been observed in this study, one of the steps in each proposed mechanism was considered irreversible. The rest of the steps were assumed to be in quasi-equilibrium. To determine the kinetic parameters of a model, the rate expression resulting from a proposed reaction mechanism was fit to the experimental data using a nonlinear least-squares algorithm. The validity of the models was judged based on the quality of the fit.

The best match between the experimental data and calculated results was obtained with the model involving dissociative adsorption of cyclohexanol on metallic copper and quasi-equilibrium between the gas and adsorbed phase cyclohexanol alcoholate and hydrogen. The formation of H_2 from cyclohexanol was assumed to occur in three sequential elementary steps, including hydrogen atom abstraction from the O–H and C–H groups and the combination of these atoms into an adsorbed hydrogen molecule. The removal of the α-hydrogen was assumed to be the irreversible, rate-determining step of the reaction. Equations (15)–(18) summarize this reaction mechanism:

$$2\text{Cu}^0 + \text{C}_6\text{H}_{11}\text{OH(gas)} \leftarrow K_{\text{CLL}} \rightarrow \text{Cu}^0\text{C}_6\text{H}_{11}\text{O} + \text{Cu}^0\text{H}, \tag{15}$$

$$\text{Cu}^0\text{C}_6\text{H}_{11}\text{O} + \text{Cu}^0 \mathrel{—} K_2 \rightarrow \text{Cu}^0\text{C}_6\text{H}_{10}\text{O} + \text{Cu}^0\text{H}, \tag{16}$$

$$\text{Cu}^0\text{C}_6\text{H}_{10}\text{O} \leftarrow 1/K_{\text{CLN}} \rightarrow \text{Cu}^0 + \text{C}_6\text{H}_{10}\text{O(gas)}, \tag{17}$$

$$2[\text{Cu}^0\text{H}] \leftarrow 1/K_{\text{H}_2} \rightarrow 2\text{Cu}^0 + \text{H}_2\text{(gas)}. \tag{18}$$

If step (16) is assumed to be irreversible and rate determining, the rate of cyclohexanone formation is given by Eq. (19)

$$R_{\text{CLN}} = LK_2\theta_{\text{CLA}}\theta\text{v}, \tag{19}$$

where L is the total number of active sites, K_2 is forward rate constant for the second step, θ_{CLA} is the fractional coverage of the catalyst by cyclohexanol alcoholate, and θv is the fraction of the active sites that are vacant. From the definition of the fractional coverage we obtain:

$$1 = \theta\text{v} + \theta_{\text{H}} + \theta_{\text{CLA}} + \theta_{\text{CLN}}. \tag{20}$$

Here, θ_{H}, θ_{CLA}, and θ_{CLN} are the catalyst fractional coverages by hydrogen, cyclohexanone intermediate, and cyclohexanone, respectively. The assumption of quasi-equilibrium in the adsorption of cyclohexanol and cyclohexanone on Cu^+ yields

$$\theta_{\text{CLA}} = K_{\text{CLL}}P_{\text{CLL}}\theta\text{v}^2/\theta_{\text{H}}^{-1/2}, \tag{21}$$

$$\theta_{\text{CLN}} = K_{\text{CLN}}P_{\text{CLN}}\theta\text{v}, \tag{22}$$

$$\theta_{\text{H}} = K_{\text{H}_2}^{-1/2}P_{\text{H}_2}^{1/2}\theta\text{v}. \tag{23}$$

Substitution of θ_{H} from (23) into (21) yields

$$\theta_{\text{CLA}} = K_{\text{CLL}}P_{\text{CLL}}\theta\text{v}/K_{\text{H}_2}^{-1/2}P_{\text{H}_2}^{1/2}. \tag{24}$$

By substituting the resulting expressions for surface coverages into Eq. (20), we obtain

$$\begin{aligned}1 = {} & \theta\text{v} + K_{\text{CLL}}P_{\text{CLL}}\theta\text{v}/K_{\text{H}}^{-1/2}P_{\text{H}_2}^{1/2} \\ & + K_{\text{CLN}}P_{\text{CLN}}\theta\text{v} + K_{\text{H}_2}^{-1/2}P_{\text{H}_2}^{1/2}\theta\text{v},\end{aligned} \tag{25}$$

$$\begin{aligned}\theta\text{v} = 1\big/\big(& 1 + K_{\text{CLL}}P_{\text{CLL}}/K_{\text{H}}^{-1/2}P_{\text{H}_2}^{1/2} \\ & + K_{\text{CLN}}P_{\text{CLN}} + K_{\text{H}_2}^{-1/2}P_{\text{H}_2}^{1/2}\big).\end{aligned} \tag{26}$$

Substitution of θ_{CLL} from Eq. (21) into Eq. (19) yields

$$R_{\text{CLN}} = LK_2K_{\text{CLL}}P_{\text{CLL}}/K_{\text{H}_2}^{-1/2}P_{\text{H}_2}^{1/2}\theta\text{v}^2. \tag{27}$$

This leads to the final rate equation:

$$\begin{aligned}R_{\text{CLN on Cu}^0} = {} & KK_{\text{CLL}}P_{\text{CLL}}/K_{\text{H}_2}^{-1/2}P_{\text{H}_2}^{1/2} \\ & \big/\big(1 + K_{\text{CLL}}P_{\text{CLL}}/K_{\text{H}_2}^{-1/2}P_{\text{H}_2}^{1/2} \\ & + K_{\text{CLN}}P_{\text{CLN}} + K_{\text{H}_2}^{-1/2}P_{\text{H}_2}^{1/2}\big)^2,\end{aligned} \tag{28}$$

where $K = LK_2$.

The best fit parameters for the constants at the three temperatures are listed in Table 1 and fits to experimental data are shown in Fig. 2. The fit is satisfactory. The activation energy of the rate-determining step, as well as the enthalpies and entropies of cyclohexanol and cyclohexanone adsorption obtained from the temperature dependence of the equilibrium adsorption constants, is presented in Table 2. The obtained kinetic model is in good agreement with IR spectroscopy results in that the cyclohexanol adsorption is dissociative and in that the removal of the second hydrogen from cyclohexanol alcoholate is the relatively slow step.

Obtained ΔS_{ads}^0 values for both cyclohexanol dehydrogenation model on Cu^+ and Cu^0 can be validated using the rules presented in [39,40]. According to these rules, ΔS_{ads}^0 must be negative and must have a magnitude smaller than the standard entropy of the vapor phase. The enthalpy of adsorption also must be negative. The values of entropy and enthalpy for cyclohexanol, cyclohexanone, and hydrogen adsorption for both models are in compliance with these rules (Table 2). The enthalpy of hydrogen adsorption on Cu^0 is close to the enthalpy value obtained for hydrogen adsorption on copper impregnated in activated carbon in [7] (-28.7 and -35 cal/(mol K) for entropy and -13.9 and -13.4 kcal/mol for enthalpy, respectively; see Table 2). Because there is no information in the literature regarding the entropy and enthalpy of cyclohexanol and cyclohexanone adsorption on copper, we compared these thermodynamic parameters with enthalpy and entropy obtained for isopropanol and acetone measured on 0.98% copper on activated carbon by Rioux and Vannice in [7]. The enthalpy and entropy of cyclohexanol adsorption are quite different from values presented in [7] for isopropanol on copper. This can be explained by the difference in the alcohol structure and the adsorption mechanism. In the current paper, the dissociative adsorption of cyclohexanol was observed, while in the case of isopropanol [7], the authors report nondissociative adsorption. At the same time, the enthalpy and entropy of cyclohexanone adsorption on Cu^0 (-14.2 kcal/mol and -25 cal/(mol K), respectively) are in good agreement with the corresponding parameters for acetone adsorption on 0.98% copper on activated carbon in [7] (-13.3 kcal/mol and -24 cal/(mol K)). This agreement reflects the fact that the adsorption mechanism is nondissociative for both ketones.

A distinguishing feature of the cyclohexanol alcoholate of Cu^+ is its very high reactivity, significantly exceeding that of the cyclohexanol alcoholate of Cu^0. Note, the electron-density shift around the copper atom should be greater in the R–O–Cu^+ group of cyclohexanol alcoholate than in the alcoholate of Cu^0.This shift in electron density also very likely affects the α-carbon reducing the electron density around it and thereby weakening the α-C–H bond. Moreover, as we noted before, cyclohexanol adsorption on the monovalent copper is accompanied by a hydrogen bond formation between the hydrogen of CH_2 group and the oxygen in the Cu^+–ZnO lattice. This interaction, even if it is weak, would speed up the removal of the second hydrogen atom by weakening the C–H bond. In the case of Cu^0, where the removal of the second hydrogen atom is the rate-determining step of the reaction, this hydrogen-boding mechanism is not available to facilitate the reaction.

5. Summary

The cyclohexanol dehydrogenation reaction over Cu–Zn–Al and Cu–Mg catalysts, formulated and pretreated to have on their surface only Cu^+ and Cu^0 surface active groups, respectively, was studied. The combined results of rate measurements and IR spectroscopy studies demonstrated:

1. Cyclohexanol dehydrogenation over monovalent copper sites proceeds through nondissociative cyclohexanol adsorption with subsequent formation of cyclohexanol alcoholate of Cu^+. The adsorbed cyclohexanol oxide is highly reactive and can be rapidly converted into cyclohexanone with no by-products. A kinetic model assuming that the abstraction of the hydroxyl hydrogen is the rate-determining step of the reaction fits the experimental reaction rate data well.
2. Cyclohexanol adsorption on zero-valent copper sites is dissociative and proceeds by the rupture of the O–H bond and formation of adsorbed species of two types: cyclohexanol alcoholate and phenolate species. These species are the intermediates for the formation cyclohexanone and phenol, respectively. The simultaneous formation of the two kinds of adsorbed intermediates makes it impossible to obtain high selectivities with Cu^0 catalysts. Unlike in the case of Cu^+-active sites, in the case of Cu^0 the abstraction of the nonhydroxylic hydrogen is the rate-determining step of the cyclohexanol dehydrogenation reaction.

References

[1] V.Z. Fridman, A.A. Davydov, J. Catal. 195 (2000) 20.
[2] Y. Takagi, S. Teratani, K. Tanaka, J. Catal. 27 (1972) 79.
[3] I. Manninger, Z. Paal, P. Tetenyi, J. Catal. 48 (1977) 442.
[4] T. Szilagyi, A. Sarkany, J. Mink, P. Tetenyi, J. Catal. 66 (1980) 191.
[5] O.N. Medvedeva, A.S. Badrian, S.L. Kiperman, Kinet. Catal. (in Russian) 17 (1976) 1530.
[6] O.N. Medvedeva, B.S. Gudkov, A.S. Badrian, S.L. Kiperman, Bull. Acad. Sci. USSR, Chem. Vers. (in Russian) 1 (1977) 19.
[7] R.M. Rioux, M.A. Vannice, J. Catal. 216 (2003) 362.
[8] U.M. Shekochihin, A.A. Davydov, The Method's Questions of Applying of IR-Spectroscopy for the Investigation of Physics-Chemistry of a Surface of Semi-conductors, N 5014-83, Vinity, Moscow, 1983.
[9] A.A. Davydov, Infrared Spectroscopy of Adsorbed Species on the Surface of Transition Metal Oxides, Wiley, Chichester, 1990.
[10] R.G. Herman, K. Klier, G.W. Simmons, B.P. Finn, J.B. Bulko, J. Catal. 56 (1979) 407.
[11] S. Menta, G.W. Simmons, K. Klier, J. Catal. 57 (1979) 339.
[12] A. Dandekar, M.A. Vannice, J. Catal. 178 (1998) 621.
[13] G. Socrates, Infrared Characteristic Group Frequencies: Table and Charts, Wiley, New York, 1994.
[14] C.J. Pouchert, The Aldrich Library of Infrared Spectra, Aldrich Chemical Co., Milwaukee, 1981.
[15] A.A. Davydov, E.M. Knyzeva, M.L. Shepotko, J. Appl. Spectrosc. (in Russian) 49 (1988) 86.
[16] L. Brabec, J. Novakova, L. Kubelkova, J. Mol. Catal. 94 (1994) 117.
[17] H.A. Pearce, N. Sheppard, Surf. Sci. 59 (1976) 205.
[18] D.M. Griffiths, C.H. Rochester, J. Chem. Soc., Faraday Trans. I74 (1978) 403.
[19] A.A. Efremov, A.A. Davydov, React. Kinet. Catal. Lett. 18 (1982) 353.
[20] V.S. Escribano, G. Busca, V. Lorinzelli, J. Phys. Chem. 94 (1990) 8939.
[21] C.I. Martin, I. Martin, V. Rives, J. Catal. 145 (1994) 239.
[22] J.L. Davis, M.A. Barteau, Surf. Sci. 208 (1989) 383.
[23] M.A. Vannice, W. Erley, H. Ibach, Surf. Sci. 254 (1991) 1.
[24] N.A. Osipova, A.A. Davydov, L.A. Kurina, V.E. Loyko, J. Phys. Chem. (in Russian) 109 (1985) 1479.
[25] N.A. Osipova, A.A. Davydov, L.A. Kurina, J. Phys. Chem. (in Russian) 109 (1985) 1484.
[26] O.V. Krylov, J. Phys. Chem. (in Russian) 39 (1965) 2911.

[27] V.B. Kazansky, E.A. Pid'ko, Kinet. Catal. (in Russian) 43 (2002) 614.

[28] F. Boccuzzi, E. Garrone, A. Zecchina, A. Bossi, M. Camia, J. Catal. 51 (1978) 160.

[29] P. Tetenyi, Z. Paal, J. Catal. 208 (2002) 494.

[30] Z. Paal, A. Peter, P. Tetenyi, Reaction. Kinet. Catal. Lett. 1 (1974) 121.

[31] I. Manninger, A. Peter, Z. Paal, P. Tetenyi, Kemiai Kozl. (in Hungarian) 44 (1975) 35.

[32] V.Z. Fridman, A.A. Davydov, J. Catal. 208 (2002) 497.

[33] M.K. Weldon, C.M. Fried, Chem. Rev. 96 (1996) 1391.

[34] D.A. Chen, C.M. Fried, Langmuir 14 (1998) 1451.

[35] A.A. Davydov, Molecular Spectroscopy of Oxide Catalyst Surface, Wiley, New York, 2003.

[36] A. Dandekar, R.T.K. Baker, M.A. Vannice, J. Catal. 184 (1999) 421.

[37] P.B. Babkova, A.K. Avetisova, G.D. Lubarskyi, Kinet. Catal. (in Russian) 11 (1970) 1451.

[38] A.I. Tripolskyi, N.V. Pavlenko, G.I. Golodez, Kinet. Catal. (in Russian) 26 (1985) 1131.

[39] M. Boudart, D.E. Mears, M.A. Vannice, Ind. Chim. Belge 32 (1967) 281.

[40] M.A. Vannice, S.H. Hyun, B. Kalpakci, W.C. Liauh, J. Catal. 56 (1979) 358.

[41] A.J. Dean, Lange's Handbook of Chemistry, fifteen edition, 1999.

[42] B.V. Erofeev, E.A. Scregan, J. Phys. Chem. (in Russian) 43 (1969) 139.